Realistic and Computational Efficient Evaluation of Temperature and Stress Development in Large RCC Dams

Jürgen Giesecke, Prof. Dr. -Ing.habil., Dr. -Ing. E. h. Director & Chairman
Institute of Hydraulic Engineering, University of Stuttgart, Germany.

Minghao Qin, PhD Student
Institute of Hydraulic Engineering, University of Stuttgart, Germany

Walter Marx, Dr.-Ing. Deputy Director
Institute of Hydraulic Engineering, University of Stuttgart, Germany.

ABSTRACT

Experience shows that temperature induced cracking is still one of the main concerns in the design and construction of RCC dams, especially in the case of large RCC dams. The special features associated with the construction of RCC dams, thin layer, large exposure area, high ascending speed as well as high content of fly ash in the cementitious materials make the temperature and thermal stress analysis for RCC dams a bigger challenge than for the conventional concrete gravity dams. Based on comprehensive studies several new methods have been proposed and adopted in an effort to develop a more realistic and computational more efficient model for the temperature and thermal stress analysis of RCC dams. The effects of material properties, climatic conditions and construction process on the distribution and development of temperature and stresses in the dam could be studied using the model.

1 INTRODUCTION

In comparison with conventional concrete dams, RCC dams have many advantages with respect to thermal cracking control. The lower potential of cracking of RCC is a result of the lower cement (on the average only 75-85 kg/m^3 [Dunstan, M.R.H.-1999]) and water content, generally lower elastic modulus and higher creep rates. Even so the thermal analysis for RCC dams is just as important as for conventional concrete dams because thermal cracks have been observed in some completed RCC dams. This is due to the following reasons:

The rapid method of construction associated with RCC dams creates an almost adiabatic behaviour of the material in the centre of the dam, as there is no time to dissipate the heat generated before placing the next layer. Because of the much bigger ratio of surface to volume of RCC dams compared with conventional concrete dams (factor 5), it is possible in RCC dams that the solar radiation contributes more heat to the structure than that generated by the cement hydration. On the other side the potential of cooling, for example due to a gentle breeze, which blows over the warm and large surface of a thin concrete lift, is also bigger. Therefore the thermal analysis for RCC dams is much more challenging than for conventional concrete dams.

The concrete lifts, which are placed at different time, have different thermal and mechanical properties as well as different boundary conditions. In order to appropriately calculate the temperature and thermal stress fields, the spatially and temporally changing material properties, boundary conditions and geometry should be considered as realistically as possible and reasonable. For this purpose numerical simulation methods based on the finite element analysis are widely used.

In traditional finite element methods the domain concerned is discretized into very small elements layer by layer, which brings about extreme high costs in computing and makes a realistic simulation for large RCC dams (H>200 m) almost unfeasible.

The main objective of this contribution is to show the main feature of the ongoing develop-

ment of a computationally effective method to analyse and calculate the transient temperature field and the related deformations and stresses in large RCC dams. With the developed method the concrete properties, construction process and climate conditions can be simulated at reasonable computing cost and more realistically.

2 CALCULATION OF TEMPERATURE FIELD

2.1 *Formulation of Heat Transfer Problem*

The spatial and temporal changing temperature field in a RCC dam can be evaluated starting from the Fourier's differential equation

(1) $$c\rho\frac{\partial T(x,t)}{\partial t}-\sum_{i=1}^{d}\frac{\partial}{\partial x_i}(\kappa_i\frac{\partial T(x,t)}{\partial x_i})=q \qquad for\ x\in\Omega, t>0$$

and in combination with the boundary and initial conditions.

In (1), $T\,[°C]$ represents the temperature, c $[J/(kg\cdot K)]$ the specific heat, ρ $[kg/m^3]$ the density; d is the dimension of the domain Ω, κ_i $[W/(m\cdot K)]$ the thermal conductivity; q $[W/m^3]$ the rate of heat generation. Boundaries with specified temperature and heat flux have been treated with the usual methods. Special attention, see below, has been given to the boundaries exposed to the open air in order to consider influence of the solar radiation and evaporation on the temperature development in RCC dams because of the large ratio of surface to volume.

2.2 *Heat Transfer on Boundaries Exposed to Open Air*

The heat exchange between the surface of a concrete structure and its environment takes place in the form of convection, radiation, conduction and possibly in the form of latent heat (evaporation and condensation). The energy balance on the surface of the structure in the open air can be approximated with

(2) $$q_n = q_H + q_L - R_n$$

in which q_n is the heat flux normal to the surface of the structure, q_H the sensible heat flux through convection and conduction, q_L the latent heat flux through evaporation and condensation and R_n net radiation. All terms are expressed in W/m^2.

2.2.1 Sensible heat flux

Sensible heat transfer, the heat exchange between structure surface and the fluid (air or water) in its environment, can be calculated with the following formula:

(3) $$q_H = \alpha_c\cdot(T_0 - T_a)$$

where $\alpha_c\,[W/(m^2\cdot K)]$ is the convective heat transfer coefficient, T_a the temperature of the fluid, and T_o the temperature of the structure surface.

2.2.2 Net radiation

Net radiation on the surface of open-air structure results from the net incoming shortwave radiation q_G and the net outgoing long-wave radiation q_E:

(4) $$R_n = q_G - q_E$$

Net incoming shortwave radiation can be calculated with

(5) $$q_G = (1.0-\alpha_G)\cdot G$$

where α_G is the albedo (reflection coefficient) of the structure surface with respect to global radiation. It varies with the texture, roughness and moisture content of the surface as well as the angle of incidence of the sun. G is the global radiation incident upon the structure surface. It can be measured on the field or estimated using solar radiation models.

The heat exchange between the structure surface and the atmosphere through long-wave (wave length >3μm) radiation can be estimated with the Stefan-Boltzmann equation

(6) $$q_E = \alpha_r \cdot (T_o - T_a)$$

(7) $$\alpha_r = \varepsilon \cdot \sigma \cdot (T_o^2 + T^2{}_a)(T_o + T_a)$$

where α_r [$W/(m^2 \cdot K)$] is the radiative heat transfer coefficient, $\sigma = 5.67035 \times 10^{-8}$ [$W/(m^2 \cdot K^4)$] the Stefan-Boltzmann constant, T_o and T_a the temperatures of the surface and the atmosphere in Kelvin, ε [-] the radiation exchange coefficient.

2.2.3 Latent heat

After RCC has been placed and compacted, the lift surface must be maintained in a damp condition. This is usually done through water spraying.

Because of RCC's large exposed lift surface, the evaporation is responsible for significant quantities of heat exchange between the lift surface and the atmosphere. This phenomenon always causes a heat loss from the concrete lift and partly balances energy from shortwave solar flux and therefore has a significant influence on the temperature field calculation.

In practice, the evaporation on newly placed concrete has been usually estimated with Menzel's formula or the ACI monograph which was derived from the Menzel formula. Because of their origin Menzel's formula and the ACI monograph are only suitable for estimating the total evaporation or the average evaporation rate over a relative long period of time. For shorter duration the actual evaporation will be notably underestimated in the hot sunny days or daytime while in cloudy days or at night notably overestimated [Hasanain, G.S.;Khallaf, T.A.; Mahamood, K., -1989]. For this reason the Penman-Brutsaert Model [Brutsaert, W. -1982], which is well approved in practice, has been used for the short time prediction of diurnal latent heat flux on wet surfaces:

From (2), (3), (4) and (6) results the heat transfer boundary condition:

(8) $$q_n = (\alpha_c + \alpha_r)(T_o - T_a) + q_L - q_G = \alpha(T_o - T_a) + q_L - q_G$$

where α_r is calculated with (7) and α_c is determined in the process of calculating q_L. q_G can be taken from the field measurements or calculated with solar radiation models. The heat transfer boundary condition (8) must be solved together with (1) step by step by means of an iterative method.

2.2 *Rate of Hydration Heat*

Hydration of concrete is a highly exothermic and thermally activated reaction. An adequate numerical simulation of the associated thermal problem requires the evaluation of the rate of hydration heat q liberated at every instant during the process. In practice, the adiabatic temperature rise T_{ad} can be measured through experiments. Assuming that the specific heat c and the density of concrete ρ keep constant during the hydration process, the rate of hydration heat q can be calculated with

(9) $$q = \dot{Q} = c\rho\dot{T}_{ad} = c\rho T_{ad}^{\infty}\dot{\xi}$$

where T_{ad} is the adiabatic temperature rise measured in the adiabatic test, and T_{ad}^{∞} the final value of T_{ad}. $\xi = {}^{T_{ad}}\!/_{T_{ad}^{\infty}}$ is the hydration degree. Under a temperature regime different from that under which T_{ad} is measured ξ can be calculated with

(10) $$\xi = \exp(-\frac{b}{t_e^n})$$

where b and n are material constants, t_e the maturity or equivalent age. The following formulation, which is equivalent to the generally accepted Arrhenius-type maturity function, is used [Carino, N.J., Tank, R.C. -1992]:

(11) $$t_e = \int_0^t \exp[B(T(\tau) - T_{ref})]d\tau$$

where B is a material constant called temperature sensitivity factor; T_{ref} the reference temperature for which maturity equals the real time. With (10) and (11) the evolution of the hydration degree $\dot{\xi}$ under a variable temperature regime can be calculated according to:

(12) $$\dot{\xi} = \frac{d\xi}{dt_e} \cdot \frac{dt_e}{dt} = bn \frac{\exp(-\frac{b}{t_e^n})}{t_e^{n+1}} \exp[B(T(t) - T_{ref})]$$

2.5 *Methods to Improve the Computing Efficiency*

RCC dams are constructed in layers of 30 to 50cm. The properties of the newly placed concrete layers change rapidly and are strongly influenced by the construction process and the environmental conditions such as air temperature, solar radiation and wind. By using traditional finite element methods, the computation domain is discretized into small elements layer by layer and small time steps are used throughout the whole construction process. Thus the construction process and the actual temperature development in a RCC dam can be well simulated. For small dams this method is still workable. But for large RCC dams the demand on hardware equipments as well as computing, hence cost, is even in 2D cases very high. In order to improve the computational efficiency, among others, the adaptive compound layer method and the adaptive time step method have been used in the ongoing work.

The adaptive compound layer method is a modified compound layer method [Zhu, B. -1994]. In the compound layer method the domain considered is divided into two regions. As the dam rises, in the newly placed layers the temperature is computed layer by layer while in the lower region, when the hydration process has almost finished and thermal and mechanical properties of the concrete of adjacent layers are not too much different from each other, these adjacent layers are combined into one layer and a coarser mesh is used. In the adaptive compound layer method the requirements for combining the layers are somewhat relaxed. For some adjacent layers, as long as the hydration degree of each layer reaches above a certain level and the thermal and mechanical properties of different layers can be linearly interpolated, these layers can be combined to form a thicker layer. The mesh size within each layer is controlled by the a posteriori estimation of the discretization error in space.

While the adaptive compound layer method controls the discretization in space, the adaptive time step method [Bornemann, F.A. -1991] controls the discretization in time. Short time steps are used in the region of sharp temperature variation (in the region of newly placed layers), and long time steps are used in the lower region of moderate temperature variation. In each region the time steps are calculated in such a way that they are adapted to the time gradient of the solution of the temperature field. This is realised through a posteriori estimation of the discretization error in time.

3 CALCULATION OF STRESS FIELD

As a result of temperature gradients and restraint conditions, thermal stress occurs and may induce cracks in concrete. Therefore, the prediction of thermal stress is very important in design and construction in order to control thermal cracking in the dam. Much work with respect to conventional mass concrete dams has been done [Giesecke, J. -1968, Marx, W. -1987].

3.1 *Aging of Concrete*

As hydration proceeds, the mechanical properties of the concrete, elastic modulus, strength and creep, change with time. Higher temperature accelerates the hydration and the aging process of the concrete. In the past, hydration degree or maturity has been widely used in

analysing the effects of the temperature on the aging process. Experimental evidence shows that the mechanical properties of the concrete depend not only on the degree of hydration but also on the kinetics of the hydration reaction. Higher curing temperature not only accelerates the development of concrete strengths but also affects the ultimate values of them. And the same temperature has different influence on the development of concrete properties at different ages. For these reasons Cervera et al [Cervera, M., Oliver, J., and Prato, T. -1999] introduced the concept of aging degree k, defined as a normalized strength of concrete:

$$f_c(k) = k \cdot f_{c,\infty} \tag{13}$$

where f_c is the compressive strength and $f_{c,\infty}$ its final value.The evolution of k depends on the evolution of the hydration degree $\dot{\xi}$ and the kinetics of the hydration reaction:

$$\dot{k} = (A_f \xi + B_f)\left({(T_T - T)} \Big/ {(T_T - T_{ref})} \right)^{n_T} \dot{\xi} \tag{14}$$

where A_f and B_f are material constants, T_{ref} is the reference temperature for the determination of f_c, T_T the maximum temperature at which hardening of concrete may occur; n_T is a material property controlling the sensibility of the compressive strength development to the curing temperature. A_f, B_f and n_T can be experimentally determined through adiabatic and compressive strength tests. $\dot{\xi}$ can be calculated with (12).

According to most codes of practice, tensile strengths and the elastic modulus can be related to the compressive strength, and therefore to the aging degree, in the following form:

$$f_t(k) = k^{2/3} f_{t,\infty}; \quad E(k) = k^{1/2} E_\infty \tag{15}$$

where $f_{t,\infty}$ and E are tensile strengths and the elastic modulus of concrete; $f_{t,\infty}$ and E_∞ are their final values.

3.2 *Strain Components in the Concrete*

The total strain ε in the concrete can be decomposed into a stress related part ε_σ and a stress unrelated part $\varepsilon_{\not\sigma}$. The stress related strain includes elastic strain ε_e and creep strain ε_c, while the stress unrelated part includes the free shrinkage ε_s and thermal strain ε_T. In the form of strain rate one has:

$$\dot{\varepsilon} = \dot{\varepsilon}_\sigma + \dot{\varepsilon}_{\not\sigma} = \dot{\varepsilon}_e + \dot{\varepsilon}_c + \dot{\varepsilon}_s + \dot{\varepsilon}_T \tag{16}$$

where a dot above each strain component denotes its first derivative with respect to time. Shrinkage strain ε_s includes temperature and moisture movement induced and autogenous shrinkage. For the thermal stress analysis of RCC dams, usually only the latter one is considered. The thermal strain ε_T can be defined in terms of the temperature and the thermal expansion coefficient α_T in the form:

$$\varepsilon_T = \alpha_T (T - T_{ref}) \tag{17}$$

with the reference temperature T_{ref} taken as equal to the temperature reached at the end of the setting phase, when the hydration degree $\xi = \xi_{set}$.

The stress related strain can be modelled with a rheologic model (Fig. 1), which consists of a spring, a Kelvin chain and a single dashpot. The material properties in the model are the stiffnesses $E(t)$, $E_i(t), i = 1, 2 \cdots, n$ and viscosities $\eta_S(t)$, $\eta_i(t), i = 1, 2 \cdots, n$. The single dashpot $\eta(S)$ is included to consider the transitional thermal creep and the long-term aging.

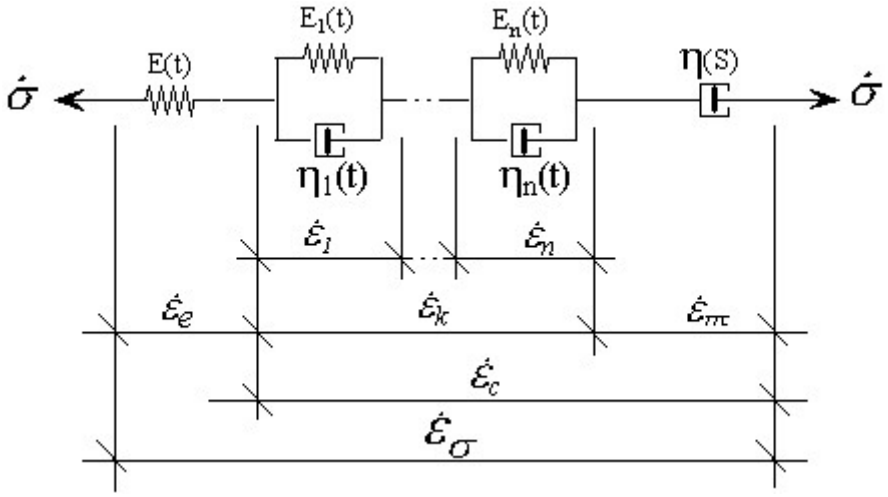

Fig. 1 Stress Related Strain Components

The influence from thermal effects on the creep properties is twofold. The first part is due to the increase in the rate of hydration with temperature that reduces the creep at higher temperatures. The second part is due to the increase in water mobility with increased temperature that reduces the viscosity of the concrete. The first part is usually considered by relating the compliance function to the hydration degree or aging degree. The second part is a function of a tensile microprestress [Bažant, Z. P., Hauggaard, A. B., Baweja, S., and Ulm, F.-J. -1997] carried by the bonds and bridges crossing micropores in the hardened cement gel:

$$\dot{\varepsilon}_{TTC} = \frac{\sigma}{\eta(S)} = c_1 S\sigma \tag{18}$$

where ε_{TTC} is the transitional thermal creep produced by the microprestress S, σ the stress, c_1 a material constant. If humidity effects are not considered, the microprestresses due to the transitional thermal effect can be estimated by solving the following equation [Hauggaard, et la.-1999]:

$$\dot{S} + c_2 S = c_3 \left|\dot{T}\right| \tag{19}$$

where c_2 and c_3 are material parameters, $\dot{T}$ denotes the change of temperature in time. c_2, c_3 and the initial value of the microprestresses can be experimentally determined.

For the *i*-th Kelvin cell (a parallelly connected strain and dashpot pair) the incremental equilibrium equation is:

$$\ddot{\varepsilon}_i + \frac{E_i(t) + \dot{\eta}_i(t)}{\eta_i(t)} \dot{\varepsilon}_i = \frac{\dot{\sigma}}{\eta_i(t)} \tag{20}$$

The creep strain rate $\dot{\varepsilon}_c$ is the sum of all the strain rates in the Kelvin chain and the transitional thermal creep rate. The stress rate can then be calculated with:

$$\dot{\sigma} = E\dot{\varepsilon}_e = E(\varepsilon - (\sum_{i=1}^{n} \dot{\varepsilon}_i + \dot{\varepsilon}_{TTC}) - \dot{\varepsilon}_s - \dot{\varepsilon}_T) \tag{21}$$

where E is the elastic modulus.

3.3 *Numerical Implementation*

An incremental procedure is adopted for the stress analysis. The time interval $[t_0, t]$ is subdivided into N time steps. With the assumption that the strain rate and material properties are constant within each time step ($t_{r-1} \le t \le t_r$), one has a closed form solution of (20). The rate form of stress-strain relation (21) can then be transformed into the following incremental form:

(22) $$\{\Delta\sigma\}_r = E_r''[\bar{D}](\{\Delta\varepsilon\}_r - \{\Delta\eta\}_r - \{\Delta\varepsilon_s\}_r - \{\Delta\varepsilon_T\}_r)$$

with

$$\frac{1}{E_r''} = \frac{1}{\bar{E}_r} + \sum_{i=1}^{n} \frac{1}{\bar{E}_{i,r}} \left[1 - \frac{1}{\Delta t_r} \frac{\bar{\eta}_{i,r}}{\bar{E}_{i,r}} \left[1 - \exp(-\frac{\bar{E}_{i,r}}{\bar{\eta}_{i,r}} \Delta t_r) \right] \right] + \frac{c_1 \bar{S}_r \Delta t_r}{2}$$

(23) $$\{\Delta\eta\}_r = c_1 \bar{S}_r \{\sigma\}_{r-1} \Delta t_r + \sum_{i=1}^{n} \frac{\{\sigma_i^d\}_{r-1}}{\bar{E}_{i,r}} \left[1 - \exp(-\frac{\bar{E}_i}{\bar{\eta}_i} \Delta t) \right]$$

$$\{\sigma_i^d\}_r = \{\Delta\sigma\}_r \frac{1}{\Delta t_r} \frac{\bar{\eta}_{i,r}}{\bar{E}_{i,r}} \left[1 - \exp(-\frac{\bar{E}_{i,r}}{\bar{\eta}_{i,r}} \Delta t) \right] - \{\sigma_i^d\}_{r-1} \left[1 - \exp(-\frac{\bar{E}_{i,r}}{\bar{\eta}_{i,r}} \Delta t) \right]$$

Here, $\bar{E}_r$, $\bar{E}_{i,r}$, $\bar{\eta}_{i,r}$ and $\bar{S}_r$ are average values of E, E_i, η_i and S in the interval ($t_{r-1} \le t \le t_r$). σ_i^d is the stress in the dashpot of the *i*-th Kelvin cell and $E_r''[\bar{D}]$ the elastic constitutive matrix.

4 NUMERICAL IMPLEMENTATION AND PRACTICAL APPLICATION

The above described methods regarding the temperature development have been implemented in the finite element program TESAR (Temperature and Stress Analysis for RCC Dams), which is partly based on Kaskade [Beck, R.; Erdmann, B.; Roitzsch, R. -1995]. The program modules for the thermal stress calculation are still under development. With TESAR the construction process and the temperature field development of Longtan RCC dam in China has been simulated and will be briefly shown here as a practical example. The required data were taken from an internal report [Yue, Y; Hu, P.; Huang, S. -1994]

4.1 *Longtan RCC Dam.*

The Longtan RCC dam is located on the upper reach of Hongshui River. The maximum dam height will be 192m in the first stage and 216.5m at the second stage. Fig.2 shows the non-overflow section of the Longtan RCC Dam. The upstream and downstream facing consist of 50 cm conventional mass concrete (CMC). The cushion layer on the bottom is 5m CMC.

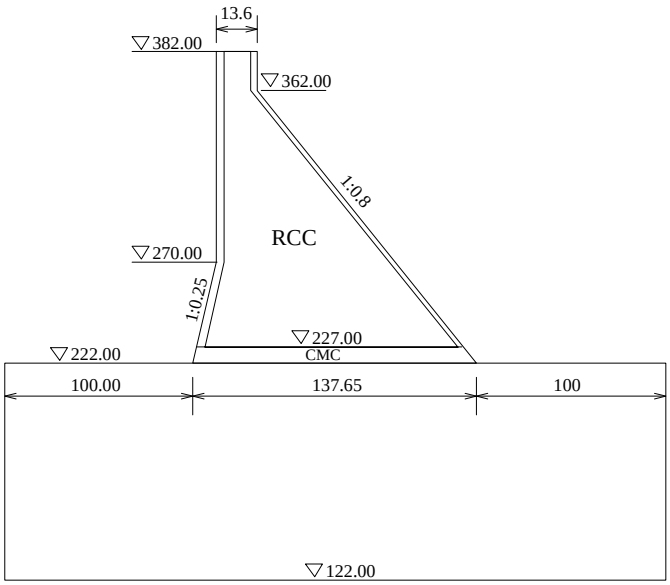

Fig. 2 Non-overflow section of Longtan RCC

4.2 *Material Properties*

4.2.1 Hydration heat

The development of hydration heat is calculated with (9), the materials constants T_{ad}^{∞}, b, n for RCC and CMC are determined thought the evaluation of the measured adiabatic temperature rise and shown in Table 1.

Table 1 Thermal Parameters for RCC and CMC in Longtan RCC Dam

Concrete type	T_{ad}^{∞}	B	N
CMC	26.8150	8.9412	0.925781
RCC	16.882	14.9621	0.871875

4.2.2 Thermal parameters

The required thermal parameters for the calculation of the temperature field of Longtan RCC Dam are listed in Table 2.

Table 2 Thermal Parameters Required for the Calculation of the Temperature Field

Parameter	Unit	RCC	CMC	Foundation
Thermal Conductivity κ	$kJ/(m\cdot h\cdot K)$	9.270	9.270	8.374
Specific Heat c	$kJ/(kg\cdot K)$	0.9673	0.9672	0.9672
Density ρ	kg/m^3	2400.0	2450.0	2400.0

4.3 *Boundary Conditions*

As shown in Fig 3, boundaries $N1$ will be regarded as adiabatic boundaries. At boundaries $C1$, $C2$, $C3$, $C4$ only the seasonal variation of the air temperature is considered. At boundary $C5$, in addition to the seasonal variation, the diurnal variation of the air temperature is also considered.

Because solar radiation measurements at the dam site are not available, the effects of solar radiation and evaporation are not considered here. Their influence on the development of the temperature field in a RCC dam will be shown below in a parametric study.

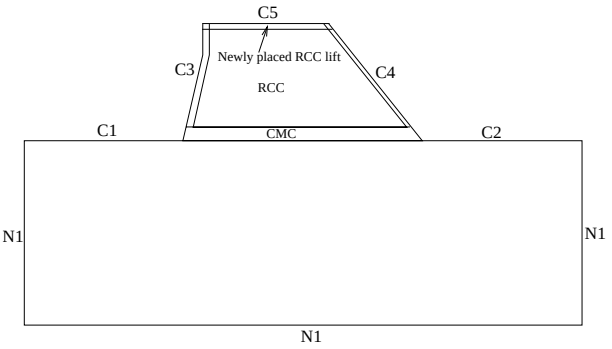

Fig. 3 Boundary Conditions

The Coefficient of surface heat transfer is $11.5\,W/(m^2\cdot K)$ for an average wind speed of $1\,m/s$ at the dam site.

4.4 *Initial Conditions*

For the placement temperature of concrete it will be assumed that it does not exceed a temperature limit T_0. If the average daily temperature is lower than T_0, the average daily temperature will be used in the simulation, otherwise T_0

4.5 *Construction Schedule*

In this simulation a construction schedule (Table 3) suggested by the designer of the Longtan RCC Dam will be used.

Table 3 Construction Schedule

Time	Elevation(m)
Feb. 1 – Apr.30 Year 5	222-227
Jun. 1. – Aug.31 Year 5	227-240
Sept. 15 – Dec.15 Year 5	240-253
Dec.16 Year 5 – Feb.15 Year 6	253-260
Feb.16 – Apr.30 Year 6	260-270
May 1 – Nov.15 Year 6	270-312
Nov 16 – Dec. 15 Year 6	312-318
Dec. 16 Year 7 – Mar. 15 Year 7	318-357
Mar. 16 – Mar. 31 Year 7	357-362
Apr.1 – May 15 Year 7	362-382

4.6 *Calculation of the Temperature Field*

For comparison, the temperature fields in the Longtan RCC Dam during construction have been calculated with program TESAR under the same conditions with the following two methods:

- Conventional method with fixed time step = 2 hours;

- Adaptive compound layer and adaptive time step method

The temperature fields at the time of the completion of concrete placement are shown in Fig.4. It can be seen that the difference of the results is negligibly small. But with the new developed method the computation time (less than 50 minutes) has been much less than that with the traditional method (about 9.5 hours).

5 IMPACT OF SOLAR RADIATION AND EVAPORATION ON RCC DAMS – A PARAMETRIC STUDY

5.1 *The 1-D Model*

In order to estimate the effects of solar radiation, wind velocity, evaporation and diurnal change of the air temperature on the temperature development in a RCC dam, a virtual RCC structure is analysed with a 1-D model.

The structure consists of 10 RCC lifts. The construction began on October 5, 1998 and was completed on October 14. A RCC lift of 50 cm thickness was placed at 7:30 each day.

5.2 *Boundary Conditions*

As in 4.3 $N1$ is the adiabatic boundary. For boundary $C5$ the solar radiation and evaporation are also considered in addition to the seasonal and diurnal air temperature fluctuation. The necessary meteorological data (air temperature, relative air humidity, sun shine duration, air pressure, wind velocity and global solar radiation) for the calculation of evaporation were taken from the Web-Service of NTUA (Department of Water Resources, Hydraulic & Maritime Engineering, National Technical University of Athen). For the period of consideration the measured global solar radiation is not complete. The missing data are supplemented through the solar radiation model. The evaporation on the concrete surface is calculated with the Penman-Brutsaert Model, provided that the RCC lift surface is kept wet all the time, i.e., that sufficient water on the lift surface is available for evaporation. The convective heat transfer between air and concrete surface is calculated iteratively during the calculation of evaporation.

5.3 *Results*

Under conditions described above, the temperature development in the structure from the construction beginning until one year after the completion of the construction is calculated. The hydration heat and other thermal parameters are the same as in section 4.2.

5.3.1 Effects of the Diurnal Changes of Air Temperature, Solar Radiation and Evaporation

The temperature development at different locations in the structure is displayed in Fig. 5. It can be observed from the figure that diurnal fluctuations of the air temperature, solar radiation and evaporation only affect the temperature near the surface of the concrete, while the cold and heat waves (lasting several days to several weeks) can influence the temperature in the structure until 2 m under the surface. Below that depth only the seasonal variations of the air temperature play a main role.

5.3.2 Effects of Solar Radiation and Evaporation

In order to show the effects of solar radiation and evaporation, three situations are considered in the calculation of the temperature development in the structure.

- Both solar radiation and evaporation are considered in the calculation;
- Only solar radiation is considered;
- Neither Solar radiation nor evaporation is considered in the calculation.

Fig.6 and Fig.7 show the temperature development under these situations. The effects of solar radiation and evaporation on the temperature evolution in RCC structures are not to overlook.

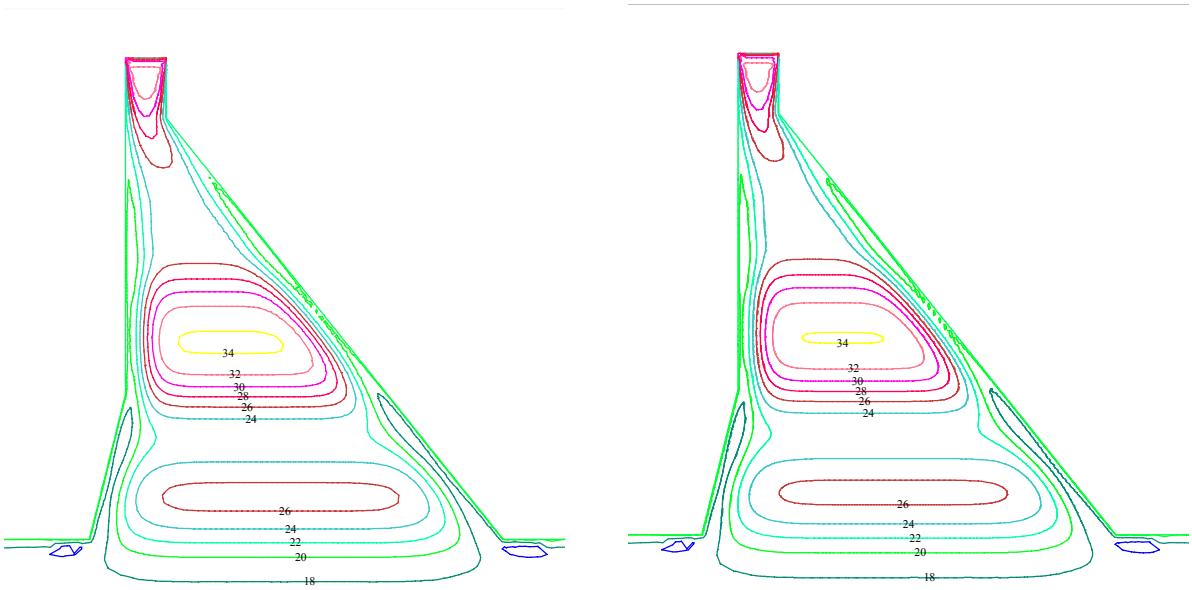

Fig. 4 Isothermal Lines of Longtan RCC Dam at the Completion of Concrete Placement, Calculated with TESAR using the Conventional Method (left) and the New Method (right)

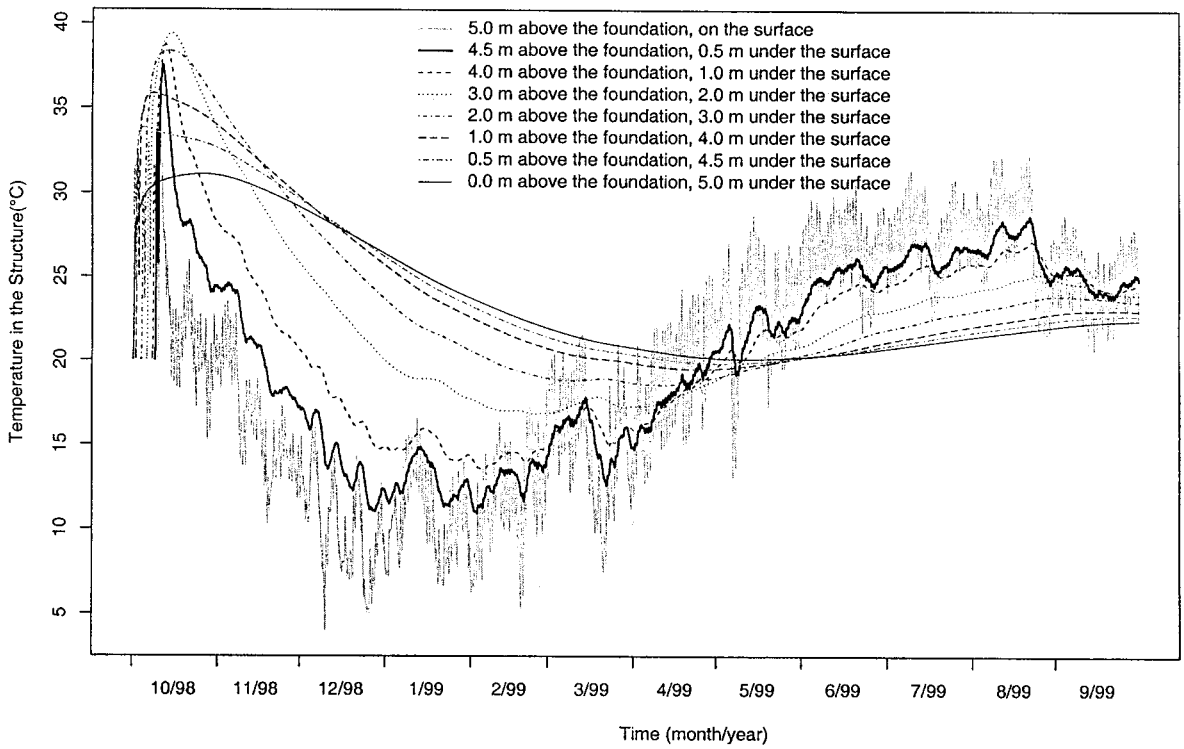

Fig. 5 Temperature Change at Different Locations During the First Year after the Completion of the Concrete Placement

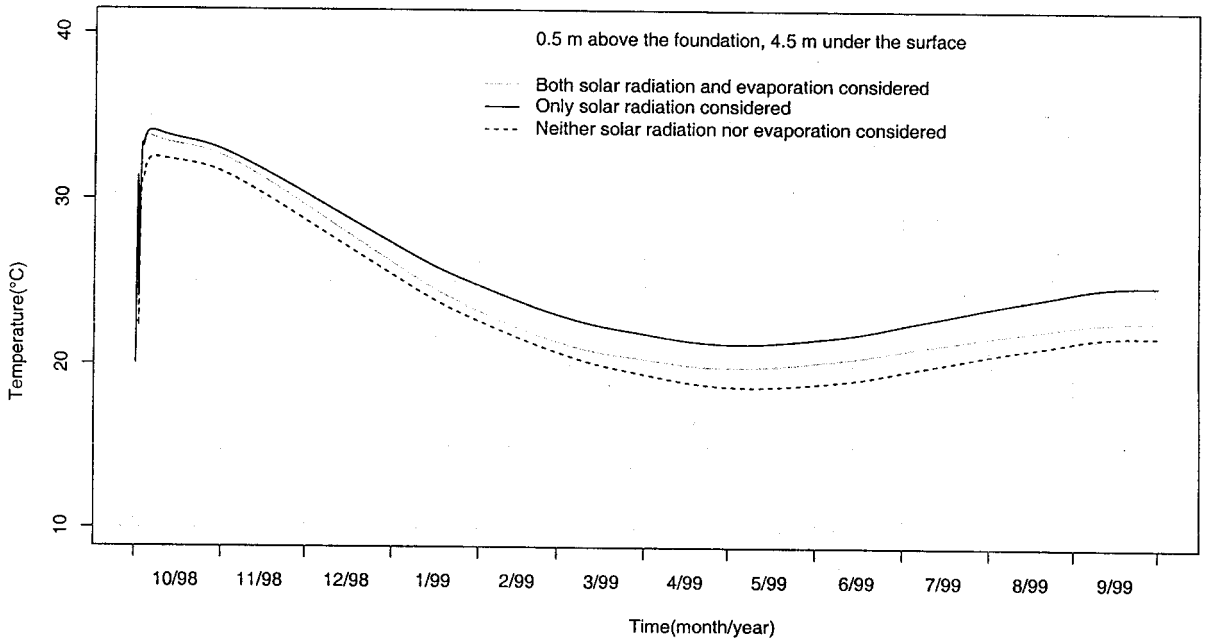

Fig. 6 Comparison of Temperature Development Calculated under Different Conditions

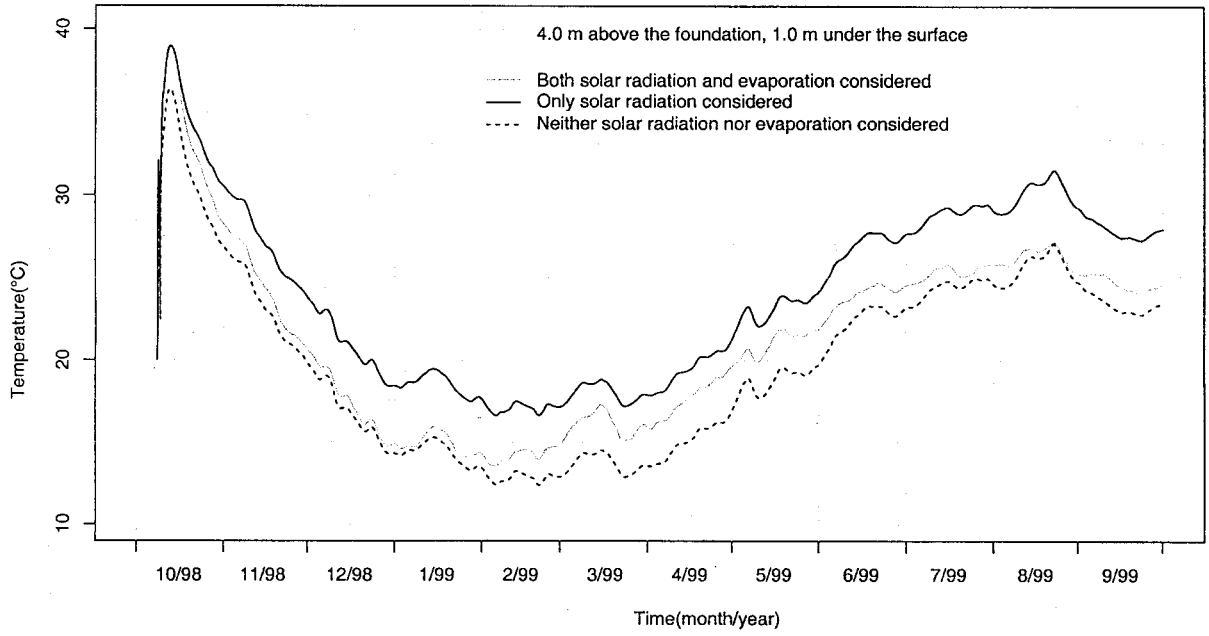

Fig. 7 Comparison of Temperature Development Calculated under Different Conditions

6 CONCLUSIONS

This paper presents some main features of the ongoing development of a computationally effective method to analyse and calculate the transient temperature field and thermal stresses in large RCC dams. Numerical procedures based on the research results have been developed and implemented in the program TESAR. With this program the construction process of a RCC Dam in China is simulated and a series of parametric studies have been conducted. The results obtained suggest the following conclusions:

The developed procedures are able to simulate the construction process and temperature development in large RCC dams efficiently and realistically. For the simulation of temperature development in RCC dams, all major influencing factors such as construction

schedule, temperature coupled hydration, solar radiation, evaporation, wind speed and air temperature are considered.

With the adaptive compound layer method and the adaptive time step method, the required computing time is only a small fraction of the time needed for the computation with the conventional method.

Because of the specific characteristics of RCC construction, the influence of the solar radiation and evaporation on temperature development is significant.

Diurnal changes of the air temperature, solar radiation and evaporation have a noticeable influence on the temperature evolution of the surface layer. Both the magnitude and distribution of the wind speed have significant effects on the temperature evolution of early age concrete.

Temperature effects on concrete creep can be considered through the concepts of maturity/aging degree and microprestresses. They are easy to implement in the numerical FE-procedure.

REFERENCES:

Bažant, Z. P., Hauggaard, A. B., Baweja, S., and Ulm, F.-J. (1997). ‘‘Microprestress-solidification theory for concrete aging and drying effects on concrete creep.’’ *J. Engrg. Mech.*, ASCE, 123, 1188–1194.

Beck, R.; Erdmann, B.; Roitzsch, R.(1995). *Kaskade 3.0 – An Object-Oriented Adaptive Finite Element Code, Technical Report TR 95-4*, June, K.Z.-Zentrum für Informationstechnik, Berlin

Bornemann, F.A.(1991). *An Adaptive Multilevel Approach to Parabolic Equations in Two Space Dimensions, Techn. Report TR 91-7*, K.Z.-Zentrum für Informationstechnik, Berlin

Brutsaert, W. (1982). *Evaporation into the atmosphere*, D. Reidel Publishing Company

Carino, N.J., Tank, R.C.(1992). Maturity Functions for Concrete Made with Various Cements and Admixtures, ACI Materials Journal, V.89, No.2, March-April, 188-196

Cervera, M., Oliver, J., and Prato, T. (1999). ‘‘Thermo-chemo-mechanical model for concrete. I: Hydration and aging.’’ *J. Engrg. Mech.*, ASCE, 125(9), 1018–1027.

Dunstan,M.R.H.(1999). “Latest development in RCC dams”, *Proc., International Symposium on Roller Compacted Concrete Dams*, Chengdu, Sichuan Prov. China, Volume I, 14-29

Giesecke, J. (1968). „Berechnung von Wärmespannungen in Massenbetonbauwerken bei linear veränderlichem Elastizitätsmodul“, *Der Bauingenieur*, 43, Heft 10.

Hauggaard, A.B.; Damkilde, L.; Freiesleben Hansen, P.(1999). “Transitional Thermal Creep of Early Age Concrete”, *Journal Of Engineering Mechanics*, April, 458-465

Hasanain, G.S.;Khallaf, T.A.; Mahamood, K. (1989). “Water evaporation from freshly placed concrete surfaces in hot weather”, *Cement and Concrete Research*. Vol. 19, 465-475

Marx, W.(1987) *Berechnung von Temperatur und Spannung in Massenbeton infolge Hydratation, Mitteilungen Institut für Wasserbau*, Universität Stuttgart, vol.64

Yue, Y; Hu, P.; Huang, S. (1994). *Thermal Stress Analysis of Water-tight Facing of Longtan RCC Dam*, Department. of Structure and Materials, IWHR, October

Zhu, B.(1994). “Compound-layer Method for Stress Analysis by Simulating the Construction Process of Multilayered High Concrete Structures”, *Journal of Hydroelectric Engineering*, Vol. 46, No.3